The Laryngoscope

Electromechanical Reshaping of Ex Vivo Porcine Trachea

Syed Hussain, BS; Cyrus T. Manuel, BS; Dmitriy E. Protsenko, PhD; Brian J. F. Wong, MD, PhD

Objectives: The trachea is a composite cartilaginous structure particularly prone to various forms of convexities. Electromechanical reshaping (EMR) is an emerging technique used to reshape cartilaginous tissues by applying electric current in tandem with imposed mechanical deformation to achieve shape change. In this study, EMR was used to reshape tracheal cartilage rings to demonstrate the feasibility of this technology as a potentially minimally invasive procedure to alter tracheal structure.

Study Design: Controlled laboratory study using ex vivo porcine tracheae.

Methods: The natural concavity of each porcine tracheal ring was reversed around a cork mandrel. Two pairs of electrodes were inserted along the long axis of the tracheal ring and placed 1.5 millimeters from the midline. Current was applied over a range of voltages (3 volts [V], 4V, and 5V) for either 2 or 3 minutes. The degree of EMR-induced reshaping was quantified from photographs using digital techniques. Confocal imaging with fluorescent live and dead assays was conducted to determine viability of the tissue after EMR.

Results: Specimens that underwent EMR for 2 or 3 minutes at 4V or 5V were observed to have undergone significant ($P < .05$) reshaping relative to the control. Viability results demonstrated that EMR reshaping occurs at the expense of tissue injury, although the extent of injury is modest relative to conventional techniques.

Conclusion: EMR reshapes tracheal cartilage rings as a function of voltage and application time. It has potential as a minimally invasive and cost-efficient endoscopic technology to treat pathologic tracheal convexities. Given our findings, consideration of EMR for use in larger ex vivo tracheal segments and animal studies is now plausible.

Key Words: Tracheal cartilage, electromechanical reshaping, shape change, cell viability.

Level of Evidence: N/A.

***Laryngoscope*, 125:1628–1632, 2015**

INTRODUCTION

The trachea is a composite structure made up of individual and incomplete cartilaginous rings. These rings are particularly prone to intraluminal convexities or abnormal curvatures of the cartilage, deformed as a result of tracheostomy tubes or previous laryngotracheal reconstructions, among other causes. Such surgical interventions can create pathologic curvatures of the tracheal cartilage that lead to debilitating stenosis.[1–4]

Current methods to treat tracheal stenosis include endoscopic dilation, stenting, cartilage grafting, and segmental resection. However, each of these procedures can be technically challenging and may fail to adequately treat the stenosis, or in rare cases (i.e., stenting) may worsen it.[2,3,5] Stenting with various plastic- or metal-based conduits can promote appropriate airflow but has been shown to cause foreign body-related reactions with prolonged usage.[4] As a result, surgical management of stenosis is associated with higher morbidity and mortality rates.[6] Laser cartilage reshaping has been shown to reshape tracheal cartilage ex vivo but at the expense of thermal injury.[7]

Electromechanical reshaping (EMR) uses electrical current delivered via needle electrodes to reshape cartilage without the need for incisions or sutures. EMR establishes localized oxidation-reduction (redox) reactions in situ, altering local tissue mechanical properties, and can be incorporated into minimally invasive delivery platforms.[8–11] Thus, EMR may be a simple and cost-efficient means to reshape tracheal cartilage rings endoscopically. This study is the first report on the use of EMR to reshape tracheal cartilage ex vivo and is the first step toward evaluating the potential use of this technology for airway convexities.

MATERIALS AND METHODS

Specimen Acquisition and Storage

Fresh ex vivo porcine tracheae, harvested from pigs approximately 90 to 110 kg in size, were obtained from a local abattoir. Between 25 and 30 incomplete "rings" of cartilage span

From the Beckman Laser Institute (S.H., C.T.M., D.E.P., B.J.F.W.); the Department of Biomedical Engineering, 3120 Natural Sciences II (B.J.F.W.), University of California Irvine, Irvine; and the Department of Otolaryngology, Head and Neck Surgery (B.J.F.W.), University of California Irvine, Orange, California, U.S.A.

Editor's Note: This Manuscript was accepted for publication January 12, 2015.

Preliminary results from this work were previously presented as an oral on February 3rd, 2013 at the International Society for Optics and Photonics West, BiOS conference (Photonic Therapeutics and Diagnostics), San Francisco, California, U.S.A.; and as a poster at the Triological Society Combined Sections Meeting, January 24–26, 2013, Scottsdale, Arizona, U.S.A.

This work was supported by the Department of Defense Deployment Related Medical Research Program (W81XWH-09-1-0602) and the National Institutes of Health (DE019026, HL103764, HL105215, EB015890). The authors have no other funding, financial relationships, or conflicts of interest to disclose.

Send correspondence to Brian J.F. Wong, MD, PhD Beckman Laser Institute, University of California Irvine, 1002 Health Sciences Road, Irvine, CA 92612. E-mail: bjwong@uci.edu

DOI: 10.1002/lary.25189

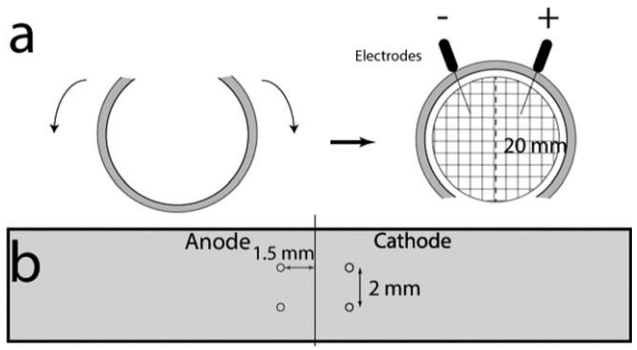

Fig. 1. (a) View of tracheal ring with concavity reversed around cork mandrel (diameter = 20 cm). (b) Lateral schematic view of the tracheal ring excised of surrounding tissues. Dashed line represents the midline of the trachea. Anodes and cathodes are 3 mm apart and 1.5 mm from the midline of the trachea. Electrodes within a paired group are 2 mm apart.

the entire length of the porcine trachea. Each omega-shaped tracheal ring is formed by three components: elastic cartilage, an inner luminal mucosal lining, and perichondrium or connective tissue on the outer surface. This composite elastic structure stretches and compresses in response to physiologic deformations.

Individual tracheal rings were sectioned free from one another. The outer perichondrium and inner mucosal luminal layer were carefully removed using microdissection techniques. Rings from the distal two-thirds of the trachea, which measured approximately 1.5 millimeters in width and 22 millimeters in diameter, were used for experimentation. As noted in previous studies, these distal tracheal rings are comparable to one another in terms of flexibility, stiffness, and size.[7] The tracheal rings were immersed in phosphate-buffered saline (PBS) at pH 7.4 and stored in a refrigerator at 5°C. All experimentation was performed within 48 hours of tissue harvest.

Electromechanical Reshaping

A digital image of each tracheal ring was taken prior to reshaping. Mechanical deformation to reverse the tracheal ring concavity was applied by wrapping the specimen around a cork mandrel and securing it with pushpins (Fig. 1a). Two pairs of platinum needle electrodes (F-E2M-48; Grass Technologies, West Warwick, RI) were inserted along the long axis, 1.5 millimeters from the midline. Needle electrodes within a paired group were separated by a distance of 2 millimeters. The electrode polarity was arranged such that the anodes and cathodes were on opposites sides of the midline (Fig. 1b). Electrode placement was determined using computational models estimating the electric field, as previously described[8,9,12]

Voltage and application time of the power supply were controlled by custom software written in Laboratory Virtual Instrument Engineering Workbench (National Instruments, Austin, TX). The dosimetry parameters chosen for this study were based on previous investigations of EMR done on porcine costal rib cartilage.[8,9,12] EMR was systematically applied to specimens using dosimetry pairs of voltages of 3 volts [V], 4V, or 5V, and application times of either 2 minutes or 3 minutes. Control specimens were mechanically deformed around the mandrel, with electrodes inserted for 3 minutes without application of electrical current. Each parameter, including the control, contained n = 8 specimens—except for 4V 2 minutes, which had 10 specimens.

Immediately after termination of voltage application, the tracheal ring specimens were immersed in PBS at ambient temperature (21°C) for 15 minutes to allow for rehydration and ionic equilibrium. The tracheal rings were maintained in deformation around the mandrel during the rehydration period. Specimens were photographed for 2 minutes after being removed from the solution and released from the jig.

Data Analysis

Measuring shape change is a complicated task with many challenges, particularly with irregular ovoid structures such as the trachea. Two methods were used to quantify shape, each focusing on a different geometric concept. The first approach measured the difference in the opening angle between pre- and post-EMR tracheal rings (Fig. 2a). The opening angle (θ) is defined by two lines that connect the incomplete ends of the tracheal ring to an apex at the midpoint of the tracheal contour. The difference between pre- and post-EMR opening angles was used to estimate the degree of shape change. The second method measures the major and minor axes of an ellipse that best approximate the shape of the tracheal ring (Fig. 2b). The axes lengths were compared before and after treatment to evaluate the widening of the airway. Differences were measured relative to the averaged pre-EMR configuration.

ImageJ (National Institute of Health, Bethesda, MD) was used to measure the opening angle, and Microsoft PowerPoint (Redmond, WA) was used to measure the elliptical axes and area. Standard t tests were performed using Microsoft Excel (Redmond, WA) to determine the variability of the results.

Confocal Microscopy

Tissue viability for each parameter was performed using laser scanning confocal microscopy (Meta 510, Carl Zeiss LSM

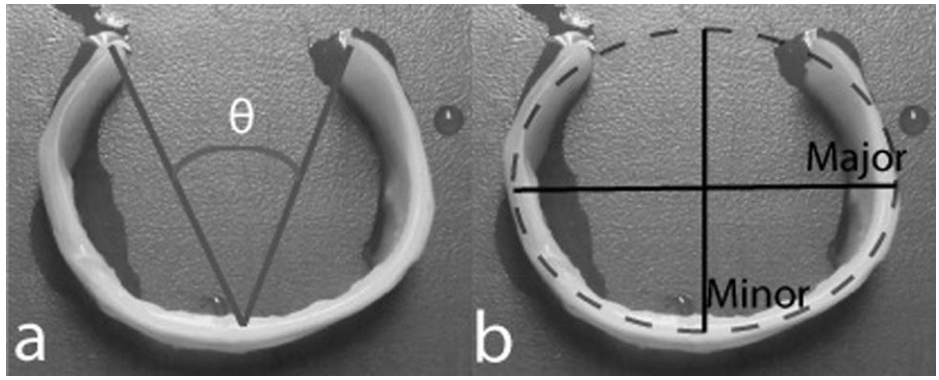

Fig. 2. Quantifying shape change: (a) opening angle measurement, and (b) major and minor axes of tracheal ellipse that best fits the tracheal ring.

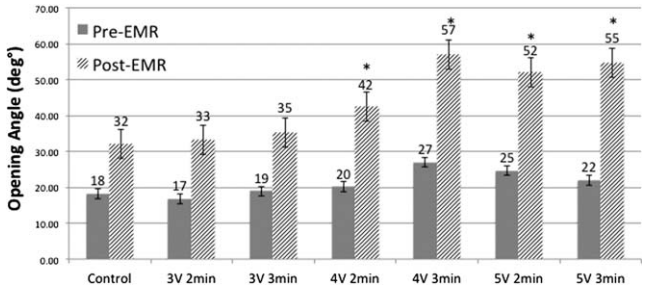

Fig. 3. Averaged absolute differences in opening angle measurement before and after EMR. All post-EMR values are statistically significant ($P < .05$) relative to their respective pre-EMR configurations. Data are mean ± SE; n = 8. *Significant difference with comparison to control ($P < .05$). EMR = electromechanical reshaping; SE = standard error.

Thornwood, NY) and the Live/Dead assay (Molecular Probes, Eugene, OR), as previously described.[7,9,10] The assay utilizes calcein AM and ethidium homodimer to differentially label live cells (green fluorescence) and dead cells (red fluorescence), respectively. The tracheal rings were prepared for the Live/Dead assay (Molecular Probes) by meticulously sectioning the specimens lengthwise with a scalpel after EMR and hydration. The lengthwise cut was made such that it bisected each needle electrode insertion hole. The specimen was then placed in the assay dye solution within a dark chamber for 30 minutes. Excess dye was washed off with PBS before being examined using confocal microscopy. Images were acquired, and a full-scale digital montage of the entire tracheal sample was created. The dimensions of nonviable (red) segments were measured using digital micrometry.

RESULTS

Electromechanical Reshaping

Post-EMR values for all parameters demonstrated significant reshaping ($P < .05$) relative to their respective pre-EMR configuration, as noted by the change in opening angles (Fig. 3). The degree of shape change increased with voltage and application time, as with other EMR studies in cartilage. Post-EMR values of parameters 4 V 2 minutes and above were observed to have significantly higher values relative to the control ($P < .05$).

The percent differences in major and minor axis length of the equivalent ellipse reflected trends similar to those observed using the opening angle as a metric (Fig. 4). Because each tracheal ring differed in its native conformation, the degree of reshaping of each ring was measured relative to its pre-EMR shape to assess shape change. Increases in voltage or application time produced wider ellipses. For example, 5V 3 minutes produced tracheal rings with average widths 22% larger post-EMR, whereas 3V 3 minutes produced rings with average widths only 11% larger. All parameters 3V 3 minutes and above were observed to have elliptical heights significantly greater relative to the control ($P < .05$).

Confocal Microscopy

Injured chondrocytes fluoresced a diffused red color at electrode insertion sites. In contrast, viable cells with bright green fluorescence were seen a small distance away from electrode insertion sites. In Figure 5, nonviable cells were depicted by a darkened gray shade localized in the centers of the samples surrounded by live cells, depicted as the bright round dots. The images demonstrate that chondrocyte injury was sharply demarcated and localized to areas immediately adjacent to the electrode insertion site. The extent of tissue injury was modest and ranged from 0.4 to 2.5 millimeters in diameter, only at the needle insertion sites (Table I). Chondrocyte injury increased with voltage and application time, as expected for all samples.

DISCUSSION

This study is the first report on the use of EMR on tracheal cartilage and demonstrated statistically significant shape change over a wide range of electrical dosimetry parameters. The onset thresholds for producing the shape change were observed from the opening-angle metric to be above 3V 2 minutes and 3V 3 minutes. Whereas an increase in either time or voltage correlates with an increasing degree of shape change, minimal shape change was observed in tracheal elastic cartilage when sustained mechanical deformation was applied (control). In contrast to previous studies on ex vivo tissue in which cartilage specimens could be precisely sectioned into uniform shapes and dimensions, differences in tracheal ring curvature, length, thickness, and width may contribute to variation in shape change outcomes. Despite the best microdissection techniques, remnant perichondrial tissue often remains attached to the rings. Furthermore, the electrical and geometrical properties of tracheal cartilage, such as thickness of the specimen, salinity, water content, and amount of luminal tissue, can all dictate the degree of shape change.[4,7,13] Regardless, the results obtained in this study of shape change as a function of voltage and application time indicate that EMR can reshape tracheal cartilage.

Reshaping appeared to plateau at higher voltages and application times (4V 3 min., 5V 2 min., 5V 3 min.). Whereas only a limited set of dosimetry parameters were used in this study, it is important to see

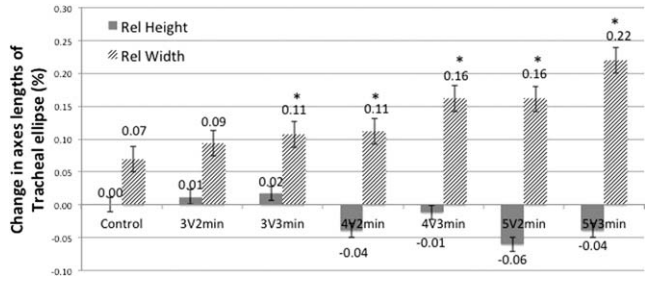

Fig. 4. Relative difference in height and width of tracheal ellipse. Each parameter is compared to itself, and results are shown as averaged percent differences. All parameters 3V 3 min. and above were observed to have elliptical heights significantly greater post-EMR relative to the control. Data are mean ± SE; n = 8. *Significant difference with comparison to control ($P < .05$). EMR = electromechanical reshaping; min. = minutes; Rel = relative; SE = standard error; V = volts.

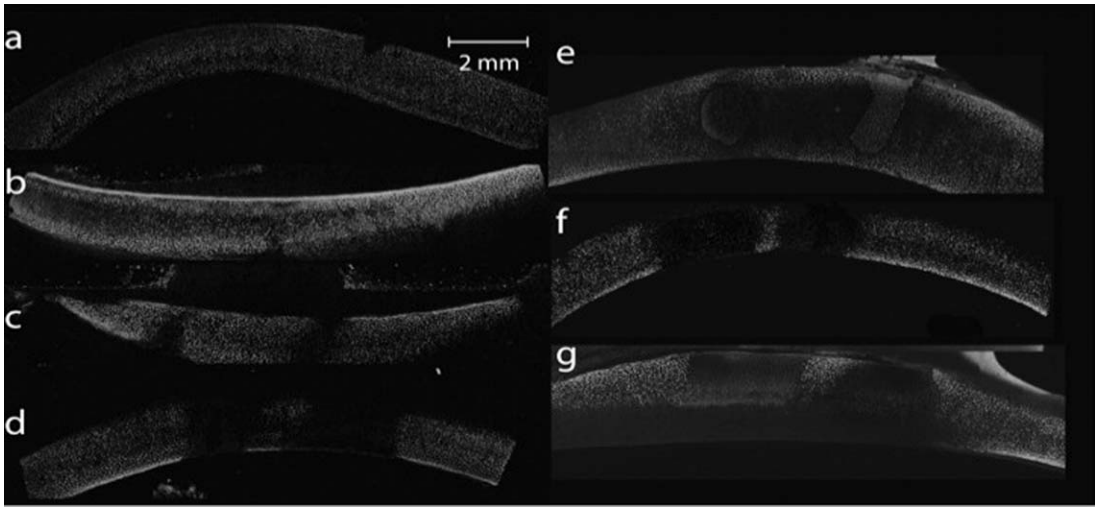

Fig. 5. Summary of confocal images of live and dead assay following treatment: (a) Control, (b) 3V 2 min., (c) 3V 3 min., (d) 4V 2 min., (e) 4V 3 min., (f) 5V 2 min., (g) 5V 3 min. Nonviable cells are visualized by the darkened gray shade localized in the centers of the samples, surrounded by live cells, visualized as the bright round dots. V = volts; min. = minutes.

parameters along a continuum and not as discrete levels. The point at which shape change saturates can be attributed to the consumption of reagents in the tissue (free water), which is limited by the diffusion of water or transport of charged moieties. An accumulation of the products of EMR, such as hydrogen ion at the anode and hydroxyl at the cathode also prevents redox reactions from occurring efficiently at the needle-tissue interface.[9,11] In a clinical setting, each case of tracheal compromise is unique, and future experiments will determine a wider range of dosimetry parameters to adequately address varying stenotic segments. Likewise, to simplify analysis, only one needle electrode pair was used, centered about the specimen midline. Future investigations will involve the use of multiple pairs distributed across the entire arc segment of the tracheal ring.

Imaging the distribution of tissue injury aids immensely in the optimization of EMR dosimetry and in the design of electrode placement geometry. The range of tissue injury varied between 0.4 and 2.5 millimeters, increasing as voltage and application time increased. Chondrocyte injury is found only adjacent to the anode and cathode and represents a small fraction of total tissue volume. This degree of tissue injury is less than that produced by conventional techniques to reshape cartilage such as morselization, crushing, or laser ablation. Although the exact mechanism by which EMR produces shape change remains unclear, it is consistent with our understanding of a faradaic process.[14] Redox reactions drive the relaxation of tissue required for shape change. The resulting pH changes at needle insertion sites are thought to be responsible for the tissue injury that accompanies EMR. As a result, the extent and type of injury necessarily differs from anode to cathode. To reduce potential tissue injury, electrodes can be inserted in patterns that reduce or distribute tissue injury, although this must be balanced with the desired degree of shape change because the EMR effect must occur with regions of increased internal stress.[9,14,15] Regardless, shape change occurs at the expense of cell injury, as expected, and success depends on the strategic spatial localization and placement of these discrete zones of tissue trauma.[9]

In our present study, we have demonstrated the feasibility of EMR in reshaping tracheal cartilage rings in terms of shape change and tissue viability. The dependence of shape change on charge transfer, the saturation of shape change at higher parameters, and minimal tissue injury sustained by chondrocytes are all expected findings of this study and in agreement with those reported in earlier investigations of EMR.[8,9,11,12,15,16] Although we have achieved our intended objectives, the relevance of the current shape change ex vivo model to clinical circumstance is rather limited. We have used tracheal cartilage that is devoid of its overlying tissues and have performed reshaping using an exaggerated geometry. We utilized larger deformations to visibly demonstrate EMR's ability to reshape tracheal cartilage in a manner that corresponds to and corroborates prior EMR work. The standardization of this EMR protocol helps establish a starting point for dosimetry selection

TABLE I.
Diameter of Red Fluorescence Around Anode and Cathode.

Parameter	Anode (mm)	Cathode (mm)
3V 2 min.	None observed	.43
3V 3 min.	.61	.71
4V 2 min.	1.17	2.31
4V 3 min.	1.64	1.51
5V 2 min.	2.04	1.29
5V 3 min.	2.52	2.38

min. = minutes; V = volts.

so that cartilage from various sources (head, neck, etc.) can be reshaped in a step-wise manner. The shape change achieved herein is not practical; however, such a preliminary study based on prior work and protocol is necessary to demonstrate the EMR effect in a preclinical setting.

The reshaping method used in this study does not reflect actual configuration that would be used in future translational studies or clinical practice. Reshaping cartilage can be done in a variety of ways (deformation geometry, electrode placement, etc.), as seen in previous reports of EMR.[8,11,15,16] Actual surgical implementation of EMR would likely only involve expansion of the stenotic segment by reshaping a flattened or ovoid structure into a rounder conduit. In practical terms, airflow through the trachea is roughly proportional to the fourth power of the effective radius at the stenotic segment. Hence, for in vivo reshaping of the trachea to be effective, dimensional changes on the order of even 1 to 2 millimeters may be adequate for therapy. Future studies will infer flow rates through the trachea using different reshaping modes.

Unfortunately, there are no reliable animal models of tracheal collapse or curvature change that simulate the conditions encountered in many adult patients. Most models produce scar and fibrosis, factors that hinder appropriate blood and electric current flow to the cartilage rather than true cartilage shape change; thus, it is difficult to translate EMR into a representative pathologic animal model. However, it is not implausible to conceive of an experimental design that attempts to expand tracheal cartilage rings in healthy animal models. These models, much like segments of tracheal convexities, would sustain blood and electric current flow to the area of deformation and allow us to observe the physiologic EMR effect, bringing our technology one step closer to a model that is minimally invasive in lieu of more expensive and traumatic surgeries.

CONCLUSION

EMR occupies a small but important niche in the possible treatment of tracheal airway obstruction with the use of needles and direct current. This system is well suited for minimally invasive, endoscopic device platforms for airway surgery. As such, it can be an alternative to current procedures in reshaping pathologic tracheal convexities as a result of previous laryngotracheal reconstructions and tracheostomies. These preliminary results are encouraging, and it seems plausible to consider using this technique next in larger ex vivo tracheal segments and animal models to bring it closer to clinical implementation.

BIBLIOGRAPHY

1. Epstein SK. Late complications of tracheostomy. *Respir Care* 2005;50:542–549.
2. Gomez-Caro A, Morcillo A, Wins R, Molins L, Galan G, Tarrazona V. Surgical management of benign tracheal stenosis. *Multimed Man Cardiothorac Surg* 2011;2011:mmcts 2010 004945.
3. Schafers HJ, Schafer CM, Zink C, Haverich A, Borst HG. Surgical treatment of airway complications after lung transplantation. *J Thorac Cardiovasc Surg* 1994;107:1476–1480.
4. Zhou W, Ding SF, Zhai Q, Wu da W. Severe tracheal stenosis due to prolonged tracheostomy tube placement: a case report. *Cases J* 2009;2: 7101.
5. Zakaluzny SA, Lane JD, Mair EA. Complications of tracheobronchial airway stents. *Otolaryngol Head Neck Surg* 2003;128:478–488.
6. Grillo HC. Stents and sense. *Ann Thorac Surg* 2000;70:1142.
7. Chae Y, Protsenko D, Holden PK, Chlebicki C, Wong BJ. Thermoforming of tracheal cartilage: viability, shape change, and mechanical behavior. *Lasers Surg Med* 2008;40:550–561.
8. Manuel CT, Foulad A, Protsenko DE, Hamamoto A, Wong BJ. Electromechanical reshaping of costal cartilage grafts: a new surgical treatment modality. *Laryngoscope* 2011;121:1839–1842.
9. Protsenko DE, Ho K, Wong BJ. Survival of chondrocytes in rabbit septal cartilage after electromechanical reshaping. *Ann Biomed Eng* 2011;39: 66–74.
10. Wong BJ, Pandhoh N, Truong MT, et al. Identification of chondrocyte proliferation following laser irradiation, thermal injury, and mechanical trauma. *Lasers Surg Med* 2005;37:89–96.
11. Wu EC, Protsenko DE, Khan AZ, Dubin S, Karimi K, Wong BJ. Needle electrode-based electromechanical reshaping of rabbit septal cartilage: a systematic evaluation. *IEEE Trans Biomed Eng* 2011;58. doi: 10.1109/TBME.2011.2157155.
12. Badran K, Manuel C, Waki C, Protsenko D, Wong BJ. Ex vivo electromechanical reshaping of costal cartilage in the New Zealand white rabbit model. *Laryngoscope* 2013;123:1143–1148.
13. Maeda K, Yasufuku M, Yamamoto T. A new approach to the treatment of congenital tracheal stenosis: balloon tracheoplasty and expandable metallic stenting. *J Pediatr Surg* 2001;36:1646–1649.
14. Protsenko DE, Ho K, Wong BJ. Stress relaxation in porcine septal cartilage during electromechanical reshaping: mechanical and electrical responses. *Ann Biomed Eng* 2006;34:455–464.
15. Yau AY, Manuel C, Hussain SF, Protsenko DE, Wong BJ. In vivo needle-based electromechanical reshaping of pinnae: New Zealand white rabbit model. *JAMA Facial Plast Surg* 2014;16:245–252.
16. Ho KH, Diaz Valdes SH, Protsenko DE, Aguilar G, Wong BJ. Electromechanical reshaping of septal cartilage. *Laryngoscope* 2003;113: 1916–1921.